INTEGRAL CORRELATION BASED OPTIMAL SD-OCT SLICE SELECTION AND PATHOLOGY CLASSIFICATION USING HANDCRAFT AND DEEP FEATURES

S. AMALADEVI[1,†], GRASHA JACOB[2]

[1]Manonmaniam Sundaranar University, Abishekapatti, Tirunelveli 627 012, Tamil Nadu, India

[2]Research Department of Computer Science, Rani Anna Government College for Women, Tirunelveli 627 008,

Tamil Nadu, India

Abstract: In this paper a novel classification system IC_HBO_DF (Integral Correlation Haar-like Biorthogonal Deep Features) for automatically classifying the retinal diseases of Age-related Macular Degeneration (AMD) and Diabetic Macular Edema (DME). The Spectral Domain Optical Coherence Tomography (SD-OCT) images are taken from the DUKE dataset that contains 15 AMD, 15 DME and 15 normal. Integral correlation function is applied to generate the optimized slices. Haar-like feature and biorthogonal approximation coefficient are extracted from the optimized slices. The convolutional neural network based pretrained GoogLeNet and VGGNet16 are used to extract the deep features from the Haar-like feature and biorthogonal approximation coefficient. Machine learning techniques Random forest, LB_Boost, DecisionTree, Adaptive_Boost are used to classify the retinal pathologies of AMD and DME. Experimental results demonstrate the effectiveness of the proposed VGGNet16 based Random forest classification algorithm that has achieved higher degree of accuracy.

Keywords: approximation coefficient; biorthogonal; convolutional neural network; correlation; Haar-like feature; random forest.

2010 AMS Subject Classification: 92B20.

———————

*Corresponding author

E-mail address: rshaamlu77@gmail.com

†Research Scholar, Register Number: 17221172162016

1. INTRODUCTION

The retina in human eye is a photosensitive layer, which transforms the focused light by the lens and converts it into neural signals and passes them to visual centre and the image is formed in the brain. The retina consists of several parts. Macula, a part of retina is located in the centre of retina and it consists of light-sensitive cells which are responsible for detecting color, light-intensity and sharp visual system. Mostly, the disorders of the macula cause the visual loss system [10]. The retina is affected by various diseases such as retinal swelling, cystoid edema, serous retinal detachment, photoreceptor layer status and atrophy. These diseases are formed by aging, diabetics, and heredity. Before changing the morphological structure of the retina, the physical symptoms are identified. Powerful techniques can be used to detect the diseases in earlier stage and diagnose these diseases or to avoid these diseases.

Spectral Domain Optical Coherence Tomography (SD-OCT) is a non-invasive real-time, high-resolution, cross-sectional biological imaging modality. It provides quantitative measurements of retinal thickness of its layer in retinal morphology, so that the ophthalmologist can easily understand the abnormal structure of the retina [6]. The most common eye diseases of macular disorders are Age-related Macular Degeneration (AMD) and Diabetic Macular Edema (DME). These are identified by the appearance of the macula.

AMD is defined by the presence of drusen, focal deposits of extracellular material and is located between the Retinal Pigment Epithelium (RPE) and the underlying choroid [1, 2] appearing dome-shaped as yellow spots in the retina. Diabetic Macular Edema (DME) is an irreversible blindness of eye disease for diabetic patients. The accumulation of exudative fluid in the macula further lead to detachment of the retinal layers and as a consequence to irreversible eye blindness [9].

In this paper, a novel classification system IC_HBO_DF is used to classify the AMD and DME of the retinal pathology is proposed.

2. LITERATURE REVIEW

In early days most of the works were mainly based on retinal layer segmentation. Retinal segmentation algorithms are different from traditional to machine learning. Srinivasan et al. [16] have presented a new automated segmenting approach using sparsity based denoising, support vector machine, graph theory and dynamic programming (S-GTDP). A. Carass et al. [5] have discussed a multi-object geometric deformation method to build layer and Random forest (RF) method to segment the nine-layer boundaries of retinal images. S.J. Chiu et al. [7] have proposed a kernel regression (KR) is used to measure the fluid and retinal layers positions. These measurements were used in graph theory and dynamic programming (GTDP) method. This was the first multi-layer accurate segmentation method used in real-world application.

Many of the works based on deep learning classification algorithms were proposed to extract the features in multi-level of abstraction and automated identification of retinal pathologies such as AMD and DME. G. Lemaitre et al. [12] have proposed an identification method for patients with diabetic macular edema using normal. SERI dataset for identification. The local binary pattern (LBP) and LBP-TOP features were used to classify the images. Five different classifiers, k-Nearest Neighbor (KNN), Logistic Regression (LR), Random Forest (RF), Gradient Boosting (GB) and Support Vector Machine (SVM) were used to classify the images. A. Albarrak et al. [2] have applied the set of local histogram-based on feature vectors to train a classifier. Bayesian network classifier was used to classify the age-related macular edema. N. Anantrasirichai et al. [3] have extracted the thickness of inner retinal layer and textural features to classify the glaucoma.

Srinivasan et al. [17] proposed a Multiscale histogram of oriented gradient descriptors as feature vector of a support vector machine learning based classifier. S.P.K. Karri et al. [11] have proposed a transfer learning based on classification of diabetic macular edema and dry age-related degeneration and healthy SD-OCT images, where CNN based pre-trained GoogLeNet was used to classify the images.

From the survey of literature, it is clear that the deep learning methods are very useful and effective, and it need a huge volume of images to reduce the over-fitting and help in constructing a generalized robust model. Through the deep learning method, extract the features very deep. In all the methods mentioned above all the image slices in the dataset are used. In the proposed IC_HBO_DF classification system is used only optimized image slices, handcraft and deep features are extracted and machine learning techniques are used to classify the retinal pathology.

3. PROPOSED METHOD

The novel classification system IC_HBO_DF is shown in Figure. 1 and described in detail in the following subsections.
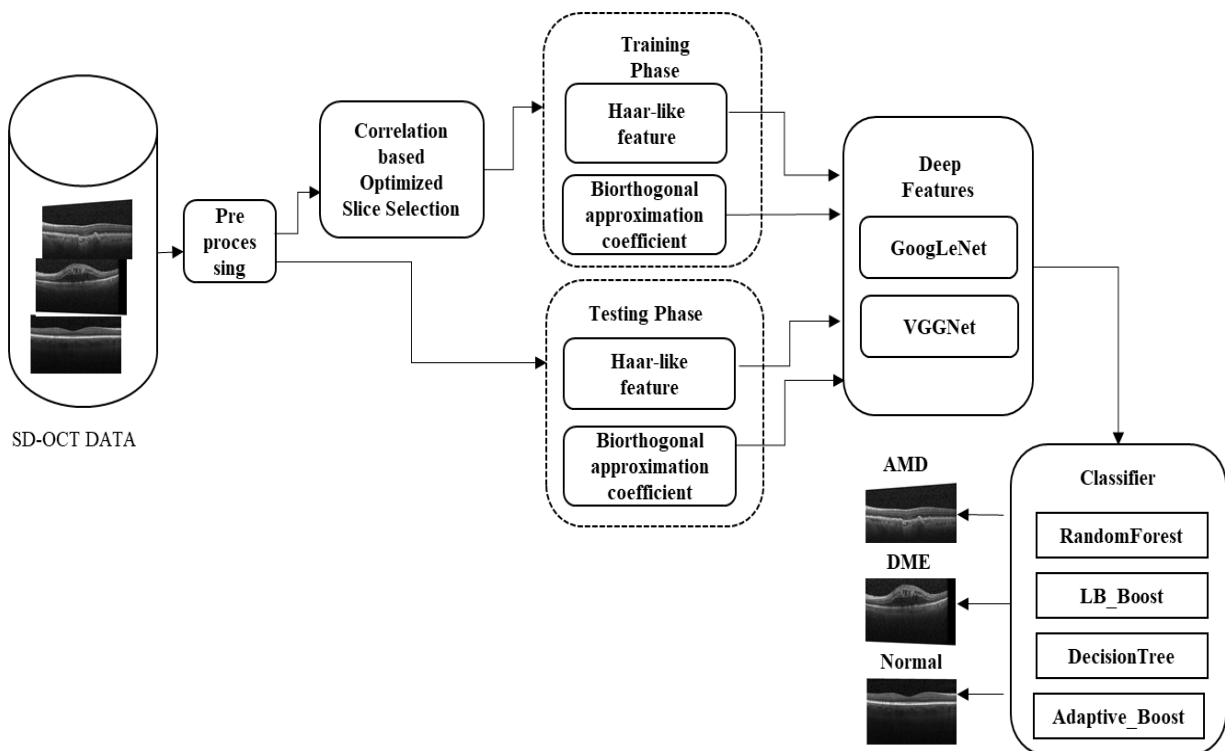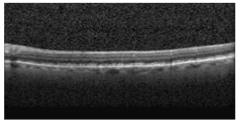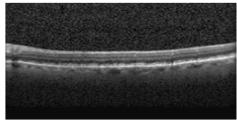

Figure 1. IC_HBO_DF classification system

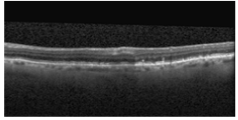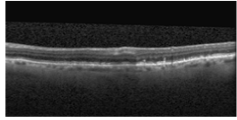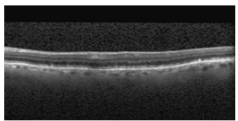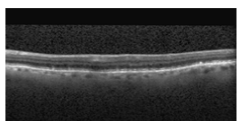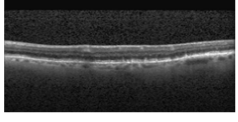## 3.1 Preprocessing:

Initially the intensity value of the image is 255. All the images are resized to 224 × 224. Block Matching and 3D(BM3D) filter are applied to produce the enhanced smooth images [8]. Once the images are filtered, the first retinal layer ILM (Inner Limiting Membrane) and the final retinal layer RPE (Retinal Pigment Epithelium) are clearly identified.

3.2 Integral Correlation based image slice selection:

IC_HBO_DF classification system selected the stack of images from the DUKE dataset [17]. There may be redundant information in the slices. Hence the proposed system to avoid this redundant information. The integral correlation based on slice selection is done in the proposed system. In this system all the preprocessed image slices are converted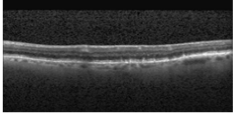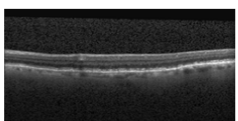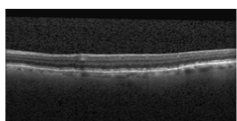 into gray images. The integral filter is applied to generate the horizontal response. First five image slices are selected from the particular subject. First image is accepted and its horizontal response is compared with the threshold value. If it is greater, then binary image is computed and this process is continued to its subsequent slice. Estimate the correlation between the first slice and its subsequent slice. The correlated value is compared with the threshold value. If greater the subsequent image is considered as similar image and rejected otherwise this image is accepted. This process is proceeded to its four subsequent slices. The correlation values of all the subsequent slices are more than the predefined threshold value means that all those five slices are in redundant form. Then this process is repeated from the fifth to its subsiding four slices once again until all the image slices of a subject and all subjects of the training images. Hence, the proposed system removes those slices in redundant for further feature extraction process apart from the first slice. Table 1 shows that the accepted and rejected image slices for a particular subject. From the table the images are clearly demonstrate those images are particularly represent the correct layer information.

Table 1. Integral Correlated Image slice selection

Image Slices	Binary Image	Correlation Value	Accepted Slices	Rejected Slices
		0.66048		
		0.63173		
		0.86835		
		0.596674		

3.3 Feature Extraction

3.3.1 Haar-like feature:

The important purpose of using features instead of pixel values as the input to the learning system to reduce the variability, and thus making the classifier easier. So, feature-based classification system works faster than pixel-based classification system. Haar-like features are mostly representing in 2-dimensional function and used to extract the anatomical structures of the objects. This is an alternate feature set instead of the usual image intensities. Haar-like features are calculated very rapidly by the integral image technique [21]. A Haar-like feature is defined as a vector $h_v = [\ t_h, h_x, h_y, h_w, h_{hi}, f\ ]$ where t_h is the type of feature, (h_x, h_y) is the left-middle point of the feature in the image h_w weight and h_{hi} height of the feature [13]. Figure. 2 (a) shows examples of the rectangle Haar-like feature. Figure. 2 (b) shows the examples of the image slice's Haar-like feature.
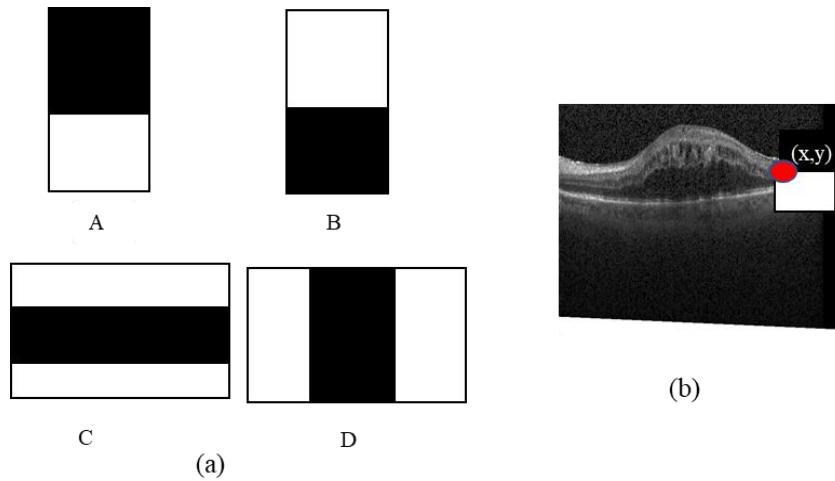
S. AMALADEVI, GRASHA JACOB

Figure 2. (a) Rectangle Haar-like feature (b) Example of Haar-like Feature

f refers to the feature value, which is defined as the difference between the sum of the intensity of all the pixels in the white region and the sum of those in the black region. The feature value f is obtained in the following equation.

$$f = \sum_{k=1}^{k} \omega^{(i)} . \mu^{(i)} \qquad (1)$$

where $\mu^{(i)}$ is the mean intensity of the pixel in image x enclosed by the ith rectangle the quantity μ represents the rectangle mean and $\omega^{(i)}$ is the weight assigned to the ith rectangle. Finally, the training and testing data of the Haar-like feature is extracted.

4. EXPERIMENTAL RESULT

Dataset:

The SD-OCT images of this system is obtained from Duke university [17] provided volumetric scans acquired from 45 patients contains 15 normal patients, 15 patients with dry AMD and 15 patients with DME using spectralis camera, and the number of b-scans per volume varies from 31 to 97 scans, each of this size is 512×496 pixels.

IC_HBO_DF Classification System

Algorithm: IC_HBO_DF Classification System

Input: SD-OCT slice SL, HR_{thr} – Horizontal Response Threshold

Output: Type AMD, DME, NORMAL

// Integral Selection $IR_{SL} \leftarrow \{\}$, HIR_{SL}

1. for each slice $sli \in SL$

2. $HR_{sli} \leftarrow$ Apply Integral Filter(sli)

3. $HRBinary_{sli} \leftarrow$ 1   if $HR_{sli} > HR_{thr}$ // Take binary image

                           0               $<= HR_{thr}$

4. $corrl_j \leftarrow correl$ ($HRBinary_{sli}$, $HRBinary_{slj}$)

5.   if (Max $corrl_j$) < 0.85

6. $IR_{SL} \leftarrow IR_{SL}$ SL_j

7. $HIR_{SL} \leftarrow HIR_{SL} \cup HR_{SLj}$

8.   end

 // Biorthogonal wavelet filter

9.   Apprcoefficient IR_{SL}

10. $APROX_{SL} \leftarrow OWT$ (IR_{SL})

11. $deep_{ortfeat} \leftarrow$ GoogLeNet ($APROX_{SL}$)

12. $deep_{HRfeat} \leftarrow$ GoogLeNet (HIR_{SL})

// Classification

13.   Trainfeat $\leftarrow$ ($deep_{ortfeattrain}$, $deep_{HRfeat}$)

14.   Testfeat $\leftarrow$ ($deep_{ortfeattest}$, $deep_{HRfeattest}$)

15.   Type $\leftarrow$ RandomForest (Trainfeat, Testfeat)

The novel IC_HBO_DF CLASSIFIER algorithm describes the detailed function of the classification   system. In this classification system, the feature extraction process consists of two phases i.e., training phase and testing phase. During the training phase the first 8 subjects from each class (AMD, DME and normal) of image slices are represented as training images. These images are self-replicated 3 times and concatenated to represent the image as 3×224×224. The integral correlation is applied to generate the redundant image slices. Haar-like feature and

biorthogonal approximation coefficient (handcraft) were extracted from the redundant training image slices. Both feature's deep features are extracted from the GoogLeNet [20] and VGGNet16 [15]. During the testing phase the remaining 7 subjects from each class of (AMD, DME and normal) of image slices represented as testing images. These images are self-replicated 3 times and concatenated to represent the image as 3×224×224. Haar-like feature and biorthogonal approximation coefficient were extracted from all the testing images. Both feature's deep features are extracted from the GoogLeNet and VGGNet16. The RandomForest, LB_Boost, DecisionTree and Adaptive_Boost machine learning techniques are used the training and testing deep features to classify the retinal pathologies as AMD, DME.

5. RESULT AND DISCUSSION

The performance of the system is evaluated by several parameters. These parameters are accuracy, sensitivity, specificity, precision and f1score. The machine learning algorithms RandomForest, LB_Boost, DecisionTree, Adaptive_Boost are used to classify the images as AMD, DME and Normal. The overall performance of the GoogLeNet and VGGNet16 based IC_HBO_DF classification system is presented in Table 2 and Table 3.

Table 2. Performance of GoogLeNet based IC_HBO_DF classification system

GoogLeNet	Accuracy	Sensitivity	Specificity	Precision	FScore
RandomForest	**0.9699**	**0.9463**	**0.9749**	**0.9597**	**0.9523**
LB_Boost	0.9522	0.9144	0.9581	0.9448	0.9267
DecisionTree	0.9565	0.9225	0.9626	0.9461	0.9323
Adaptive_Boost	0.9632	0.9353	0.9708	0.9472	0.9401

Table 3. Performance of VGGNet16 based IC_HBO_DF classification system

VGGNet-16	Accuracy	Sensitivity	Specificity	Precision	Fscore
RandomForest	**0.9885**	**0.9842**	**0.9913**	**0.9817**	**0.9829**
LB_Boost	0.9871	0.9815	0.9904	0.9793	0.9803
DecisionTree	0.9866	0.9818	0.9902	0.9777	0.9797
Adaptive_Boost	0.9881	0.984	0.9911	0.9804	0.9822

All the quantitative metric values of both Table 2 and Table 3 observed that RandomForest [4] technique performs better than the other techniques and VGGNet16 have obtained better performance than GoogLeNet. The experimental results clearly indicate that the VGGNet16 based RandomForest have achieved the higher performance than the other techniques. Experimental performance comparison of VGGNet16 and GoogLeNet based IC_HBO_DF system metrics are clearly represented graphically in Figure 3 Accuracy, Figure 4 Sensitivity, Figure 5 Specificity, Figure 6 Precision, and Figure 7 FScore.
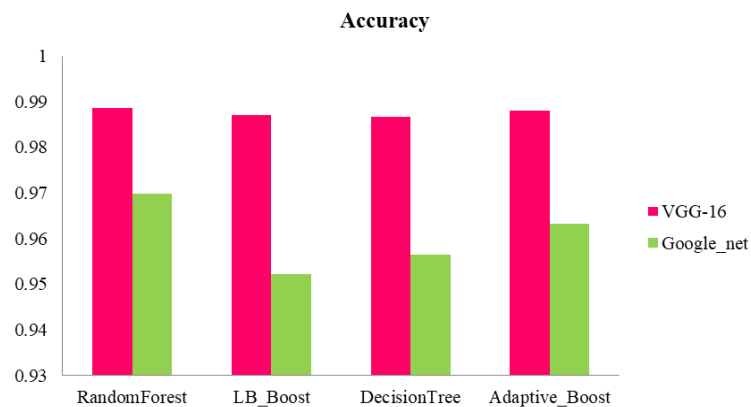
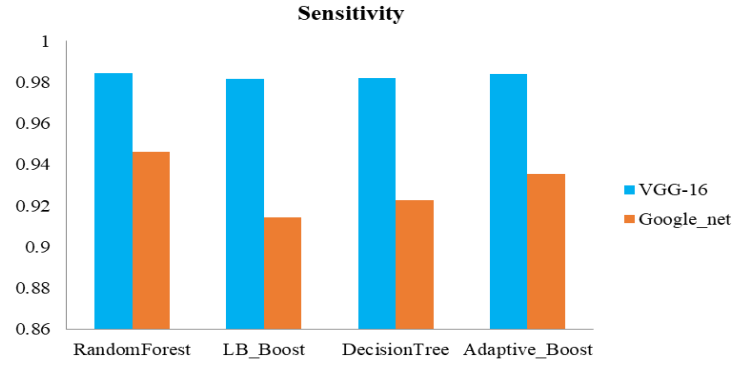Figure 3. Performance metric accuracy of VGGNet16 with GoogLeNet

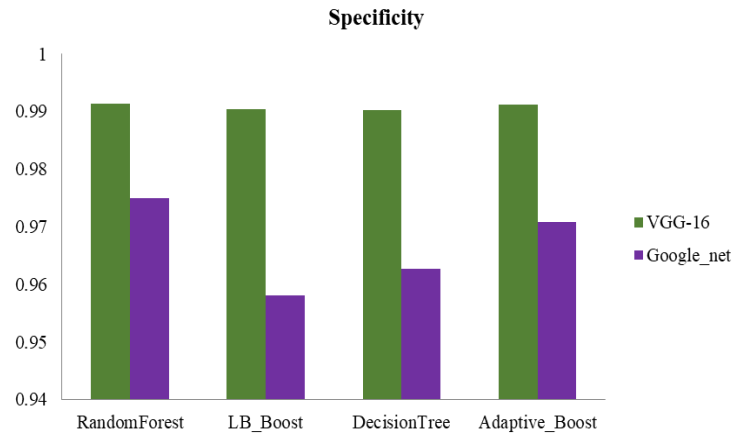Figure 4. Performance metric sensitivity of VGGNet16 with GoogLeNet

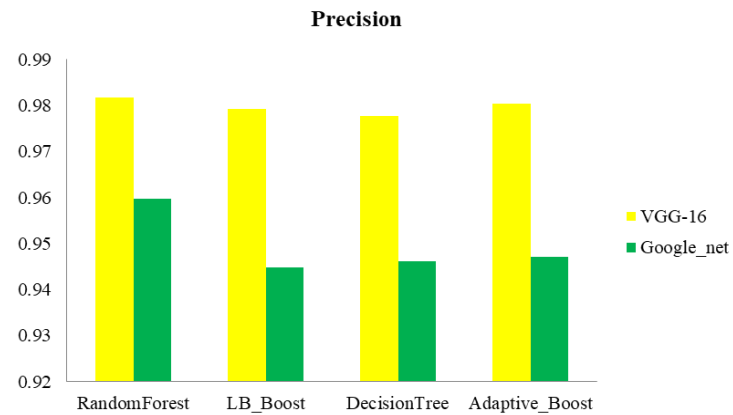Figure 5. Performance metric specificity of VGGNet16 with GoogLeNet

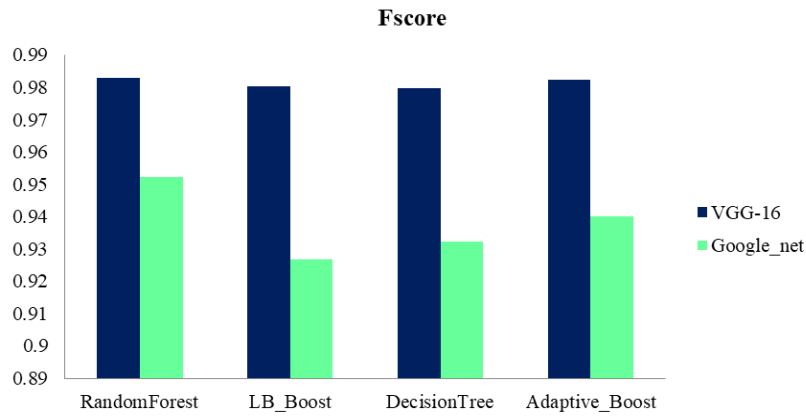Figure 6. Performance metric precision of VGGNet16 with GoogLeNet

Figure 7. Performance metric F1score of VGGNet16 with GoogLeNet

Table 4. Performance comparison of IC_HBO_DF system with S.P.K. Karri

Metric	S.P.K. Karri	IC_HBO_DF
Sensitivity	91.33	98.42

Table 4. shows the performance comparison of VGGNet16 based IC_HBO_DF classification system have obtained the overall sensitivity 98.42, which is better than the S.P.K. Karri et al.,[11] transfer learning model have obtained 91.33.

5. CONCLUSION

In this paper, propose a novel IC_HBO_DF approach automatically classify the retinal pathologies in AMD, DME and normal. In this system correlation function is used to obtained the optimized image slices. From these slices handcraft features of Haar-like and biorthogonal approximation coefficient are extracted. Convolution neural network based GoogLeNet and VGGNet16 are used to extracted the deep features. Experimental performance of the system demonstrates that both of these handcraft and deep features give the best results in all the metric

values. VGGNet16 have obtained better performance than GoogLeNet. The experimental results clearly indicate that the VGGNet16 based RandomForest have achieved the higher performance than the other techniques.

CONFLICT OF INTERESTS

The author(s) declare that there is no conflict of interests.

REFERENCES

[1]   A. Abdelsalam, L. Del Priore, M.A. Zarbin, Drusen in Age-Related Macular Degeneration, Surv. Ophthalmol. 44 (1999), 1–29.

[2]   F. Albarrak, Coenen, and Y. Zheng, Age-related Macular Degeneration Identification in Volumetric Optical Coherence Tomography Using Decomposition and Local Feature Extraction, in 17th Annual Conference in Medical Image Understanding and Analysis (MIUA), (2013), 59–64.

[3]   N. Anantrasirichai, A. Achim, J.E. Morgan, I. Erchova, L. Nicholson, SVM-based texture classification in Optical Coherence Tomography, in: 2013 IEEE 10th International Symposium on Biomedical Imaging, IEEE, San Francisco, CA, USA, 2013: pp. 1332–1335.

[4]   L. Breiman, Random forests, Mach. Learn. 45 (2001), 5–32.

[5]   A. Carass, A. Lang, M. Hauser, P.A. Calabresi, H.S. Ying, J.L. Prince, Multiple-object geometric deformable model for segmentation of macular OCT. Biomed. Opt. Express. 5 (2014), 1062–1074.

[6]   T.C. Chen, B. Cense, M.C. Pierce, et al. Spectral Domain Optical Coherence Tomography: Ultra-high Speed, Ultra-high Resolution Ophthalmic Imaging, Arch Ophthalmol. 123 (2005), 1715-1720.

[7]   S. J. Chiu, M.J. Allingham, P.S. Mettu, et al. Kernel regression-based segmentation of optical coherence tomography images with diabetic macular edema, Biomed. Opt. Express, 6(4) (2015), 1172-1194.

[8]   K. Dabov, A. Foi, V. Katkovnik, K. Egiazarian, Image denoising by sparse 3-D transform-domain collaborative filtering, IEEE Trans. Image Process. 16 (2007), 2080-2095.

[9]   G.E. Lang, Diabetic Macular Edema, Ophthalmologica. 227 (2012), 21–29.

[10] G.D. Hildebrand, A.R. Fielder, Anatomy and Physiology of the Retina, in: J. Reynolds, S. Olitsky (Eds.), Pediatric Retina, Springer Berlin Heidelberg, Berlin, Heidelberg, 2011: pp. 39–65.

[11] S.P.K. Karri, D. Chakraborty, J. Chatterjee, Transfer learning-based classification of optical coherence tomography images with diabetic macular edema and dry age-related macular degeneration, Biomed. Opt. Express. 8(2) (2017), 579-592.

[12] G. Lemaitre, M. Rastgoo, J. Massich, C. Y. Cheung, T. Y. Wong, E. Lamoureux, D. Milea, F. Meriaudeau, and D. Sidibe, Classification of SD-OCT volumes using local binary patterns: Experimental Validation for DME detection, J. Ophthalmol. 2016 (2016), 3298606.

[13] D. Ni, X. Yang, X. Chen, C.-T. Chin, S. Chen, P.A. Heng, S. Li, J. Qin, T. Wang, Standard Plane Localization in Ultrasound by Radial Component Model and Selective Search, Ultrasound Med. Biol. 40 (2014), 2728–2742.

[14] J.S. Schuman, C.A. Piliafito, J.G. Fujimoto and J.S. Duker, Optical Coherence Tomography of Ocular Diseases. 3rd ed. Slack Inc., New Jersey,2013.

[15] K. Simonyan, A. Zisserman, Very Deep Convolutional Networks for Large-Scale Image Recognition, ArXiv:1409.1556 [Cs]. (2015).

[16] P.P. Srinivasan, S.J. Heflin, J.A. Izatt, V.Y. Arshavsky and S. Farsiu, Automatic segmentation of up to ten-layer boundaries in SD-OCT images of the mouse retina with and without missing layers due to pathology, Biomed. Opt. Express. 5(2) (2014), 348-365.

[17] P.P. Srinivasan, L.A. Kim, P.S. Mettu, S.W. cousins, G.M. comer, J.A Izatt, Fully automated detection of diabetic macular edema and dry age- related macular degeneration from optical coherence tomography images, Biomed. Opt. Express. 5(10) (2014), 3568-3577.

[18] G. Staurenghi, S. Sadda, U. Chakaravarthy, R.F. Spaide, Lexicon for anatomic landmarks in normal posterior segment spectral-domain optical coherence tomography, Ophthalmology. 121(8) (2014), 1572-1578.

[19] Y. Sun, S. Li, Z. Sun, Fully automated macular pathology detection in retinal optical coherence tomography images using sparse coding and dictionary learning, J. Biomed. Opt. 22 (2017), 016012.

[20] Szegedy, W. Liu, Y. Jia, P. Sermanet, S. Reed, D. Anguleoy, D. Erhan, V. Vanhoucke and A. Rabinovich, Going deeper with convolutions, in Proceedings of the IEEE Conference on Computer Vision and Pattern Recognition, (2015), 1-9.

[21] P. Viola, M. Jones, Robust real-time face detection, Int. J. Computer Vision, 57(2) (2004), 137-154.

[22] Y. Wang, Y. Zhang, Z. Yao, R. Zhao, F. Zhou, Machine learning based detection of age-related macular degeneration (AMD) and diabetic macular edema (DME) from optical coherence tomography (OCT) images, Biomed. Opt. Express. 7(12) (2016), 4928-4940.